Surfactant adsorption and transport onto a foam lamella in a foam fractionation column with reflux

Denny Vitasari
Chemical Engineering Department
Universitas Muhammadiyah Surakarta
denny.vitasari@ums.ac.id

Paul Grassia
School of Chemical Engineering
and Analytical Science
The University of Manchester

Peter Martin
School of Chemical Engineering
and Analytical Science
The University of Manchester

***Abstract*—The adsorption and transport of surface active material such as surfactant and/or protein onto the surface of a lamella in a foam fractionation column with reflux is investigated using mathematical simulation. The dynamics of adsorption of protein and/or surfactant from the bulk solution onto the surface of the foam lamella is modelled using the Ward-Tordai equation combined with relevant adsorption isotherms such as the Henry, Langmuir or Frumkin isotherms. Once the surface active material is attached to the surface of the lamella and the surface of the Plateau border, the transport of that material (in this study is represented by surfactant in the first instance) is modelled based on the continuity equation. There are two approaches to the transport of surfactant discussed in this study. One is the transport of surfactant onto a foam lamella in the absence of surface viscosity and in the presence of film drainage. The second approach to the transport of surfactant onto a foam lamella includes the surface viscosity, however the effect of film drainage is neglected to simplify the problem thus the model provides a benchmark for a more complicated system that would involve film drainage.**

Competition between protein and surfactant may occurs in the absorption of mixed protein-surfactant. The protein arrives onto the interface at a later time due to a slower diffusion rate and it displaces the surfactant molecules already on the surface since protein has a higher affinity for that surface than surfactant. In the absence of surface viscosity, the Marangoni effect dominates the film drainage results in accumulation of surfactant on the surface of the foam lamella in the case of a lamella with a rigid interface. In the case of a film with a mobile interface, the film drainage dominates the Marangoni effect and surfactant is washed away from the surface of the lamella. When the drainage is very fast, such as that which is achieved by a film with a mobile interface, the film could be predicted to attain the thickness of a common black film, well within the residence time in a foam fractionation column, at which point the film stops draining and surfactant starts to accumulate on the lamella surface. The desirable condition in operation of a foam fractionation column however is when the Marangoni effect dominates the film drainage and surfactant accumulates on the surface of a foam lamella such as the one achieved by film with a rigid interface. In the presence of surface viscosity and the absence of film drainage, the surface viscous forces oppose the Marangoni effect and reduce the amount of surfactant transport onto the foam lamella. A larger surface viscosity results in less surfactant transport onto the foam lamella.

Keywords: **foam fractionation, adsorption, surfactant transport, film drainage, foam film**

I. Introduction

Foam fractionation is an economical and environmentally friendly separation method for surface active material such as protein and/or surfactant [1], [2], [3], [4], [5] based on bubble separation techniques [6]. Although recently there are significant number of application-related research on foam fractionation column followed by vast number of publication, the commercial application of the technique is very limited [7]. Foam in a foam fractionation column consists of air bubbles separated by thin liquid films [8]. Due to its amphiphilic nature, the surface active material is adsorbed onto the surface of the bubbles [9]. Since air bubbles have much lower density than the liquid, they will be lifted up to the top of the column carrying the surface active material with them. The enriched foamate is then collected from the top of the column. The amount of adsorbed material determines the efficiency of a foam fractionation column [1]. The adsorbed materials also have a role to stabilise the liquid film, preventing the bubble coalescence and foam collapse [10], [11], [12], [13] by reducing the mobility of the film surface [11]. The design of a foam fractionation process needs to optimise the efficiency of the adsorption as well as the stability of the foam.

Protein and surfactant may coexist in commercial foam separations [9] depending on the nature of the solution and also when there is modification of the solution to improve its separation efficiency [14], [9], [15]. Surfactant is mixed with protein to modify the adsorption as well as the rheological characteristic of the adsorbed protein layer [16], [17], [18]. When adsorbed on the interface, protein may exhibit an immobile surface that stabilize the liquid film [14], [9]. On the other hand, surfactant may form a mobile interface that may stabilize the film later on due to the Gibbs-Marangoni effect [9]. When those two components coexist in a foam film, the effect may be different from that which results from the pure substance [9]. Protein and surfactant molecules may also compete to occupy the interface [19], [17]. Therefore, it is important to study the adsorption behaviour of mixed protein-surfactant in order to estimate the efficiency of a foam fractionation column as well as the stability of the foam itself.

Due to low liquid content within the foam (less than 10%), the air bubbles take polyhedral shapes [20], separated by thin liquid film named foam lamella [8]. Three films meet and form an interstitial channel named Plateau border [21], [8]. Most of the liquid within a foam is contained in the Plateau borders [21] and connected into a network within the foam. Due to the curvature of the Plateau border, the pressure within it is lower than that in the film [22]. As a consequence, there will be liquid drainage from the film towards the Plateau border [22], [23].

Some foam fractionation columns employ a reflux system to improve the enrichment of the rising liquid [6], [24], [25], by returning some part of the collapsed foamate to the top of the column. The rising stream from the bottom of the column is enriched by the falling stream from the top [24]. As falling stream drains through the Plateau border network, it exchanges mess with adjacent films. This enrichment takes place within the Plateau borders since most of the liquid within a foam is inside the Plateau border. As a consequence, the concentration of surface active material in the Plateau border is higher than that in the foam film.

Studies on the film drainage and its effect on foam and foam film stabilisation have been carried out [23], [26], [22], [27], [11], [28], [29]. However, those studies only consider the film thinning and did not explore the transport of surfactant onto the foam lamella. On the other hand, the transport of surfactant onto the surface of the foam lamella due to the interaction of forces on it also plays an important role in determining the separation efficiency of a foam fractionation column. Therefore, this study examines the transport of surfactant onto the foam lamella and the phenomena involved in that transport. Those phenomena include the film drainage, the Marangoni forces and the viscous forces that arise in response to the resultant of other forces.

The purpose of a foam fractionation column is to separate surface active materials from the solution by attachment of those materials onto the surface of the air bubbles. Therefore, studying the dynamics and equilibrium of adsorption of surface active material onto the foam as well as the transport of that surface active material onto the foam film is fundamental for predicting the efficiency of a foam fractionation column. The knowledge of adsorption and transport of surface active materials onto a foam film will be useful to model the whole foam fractionation column system. In this study, foam fractionation column with reflux is selected as it gives a better separation efficiency.

II. Adsorption of mixed protein-surfactant

There are many studies examining the kinetics of adsorption of mixed protein-surfactant. Those studies [30], [16], [31], [19], [32] determine the adsorption dynamics as well as adsorption isotherms of mixed protein-surfactant on a bubble surface based on experimental data. Studies on the mathematical modelling of adsorption behaviour of mixed protein surfactant are less common. A *predictive* mathematical model for the adsorption dynamics and adsorption isotherm of mixed protein-surfactant has a significant importance for examining the efficiency of a foam fractionation column. Using mathematical model, the cost of conducting experiments can be minimised without losing the important information on the adsorption behaviour. Therefore, this study aims to develop a mathematical model for adsorption of mixed protein-surfactant on a bubble surface that can be applied to determine the efficiency of a foam fractionation column.

The equation of state of the surface layer then can be presented as follows [33]:

$$-\frac{\Pi\omega_0}{RT} = \ln(1-\theta_p-\theta_s)+\theta_p(1-\omega_0/\omega_p)+\alpha_p\theta_p^2+\alpha_s\theta_s^2+2\alpha_{ps}\theta_p\theta_s \quad (1)$$

where $\Pi = \gamma_0 - \gamma$ is the surface pressure, γ_0 is the surface tension of the solvent, γ is the surface tension of the solution, R is the gas law constant, T is the temperature, $\theta_p = \omega_p\Gamma_p$ is the protein surface coverage fraction, Γ_p is the total adsorption of protein, ω_p is the average molar area of the adsorbed protein molecules, $\theta_s = \omega_s\Gamma_s$ is the surfactant surface coverage fraction, ω_s is the molar area of the adsorbed surfactant, Γ_s is the surface concentration of surfactant, ω_0 is the molar area of the solvent, α_p is the intermolecular interaction parameter of protein, α_s is the intermolecular interaction parameter of surfactant, α_{ps} is a parameter describing the interaction between the protein and surfactant mixture. The adsorption isotherm of the protein is then derived as:

$$b_pC_p = \frac{\theta_p}{(1-\theta_p-\theta_s)}\exp[-2\alpha_p\theta_p - 2\alpha_{ps}\theta_p] \quad (2)$$

where C_p is the concentration of the protein in the subsurface layer and b_{pi} are the equilibrium adsorption constants of protein in the state i.

The adsorption isotherm equation for the surfactant is analogous as follows:

$$b_sC_s = \frac{\theta_s}{(1-\theta_p-\theta_s)}\exp[-2\alpha_s\theta_s - 2\alpha_{ps}\theta_p] \quad (3)$$

where C_s is the concentration of the surfactant in the subsurface layer and b_s is the equilibrium adsorption constant of surfactant.

Adsorption dynamics of both protein and surfactant towards the gas-liquid interface follow Fick's equation [34], [35]. The Laplace transformation of the diffusion equation results in a general dynamics of adsorption equation on a liquid-gas interface as proposed by Ward and Tordai [36]. The equation describes the evolution of surface concentration due to transfer from the subsurface as follows:

$$\Gamma_p(t) = \sqrt{\frac{D_p}{\pi}}\left[2C_{pb}\sqrt{t} - \int_0^t \frac{C_p(\tau)}{\sqrt{t-\tau}}\mathrm{d}\tau\right] \quad (4)$$

$$\Gamma_s(t) = \sqrt{\frac{D_s}{\pi}}\left[2C_{sb}\sqrt{t} - \int_0^t \frac{C_s(\tau)}{\sqrt{t-\tau}}\mathrm{d}\tau\right] \quad (5)$$

where D_p and D_s are diffusion coefficients of protein and surfactant in the solvent, respectively, C_{pb} and C_{sb} are the bulk

concentrations of protein and surfactant, respectively and τ is a dummy integration variable. The first term on the right hand side of the equation represents the diffusive transport to the surface. This diffusion is mitigated by a reduction in diffusive driving force as surfactant and/or protein on the surface builds up, which is presented by the second term of the right hand side of the equation. The Ward-Tordai equation presented in Equations $4-5$ is applicable on a planar interface. This shape of interface is selected as in common applications such as foam fractionation, polyhedral bubbles with nearly planar films occur in the system, due to low fraction of liquid [21].

A dimensional analysis is carried out upon the equations of dynamics of adsorption of mixed protein-surfactant which are Equations 2, 3, 4 and 5. The dimensionless form of the equations governing the dynamics of adsorption involves dimensionless groups that we call $\mathcal{D}$, Γ_m, κ_p, κ_s and c_b, precise definitions of which will be given shortly. The resulting dimensionless equations are as follows.
Dynamics of protein adsorption:

$$\theta_p(t') = \frac{1}{\sqrt{\pi}}\left[2\sqrt{t'} - \int_0^{t'} \frac{C_p'(\tau')}{\sqrt{t'-\tau'}}\mathrm{d}\tau'\right] \tag{6}$$

Adsorption isotherm of protein:

$$C_p'(t') = \frac{\theta_p(t')}{\kappa_p\left[1-\theta_p(t')-\theta_s(t')\right]}\exp\left[-2\alpha_p\theta_p(t') - 2\alpha_{ps}\theta_s(t')\right] \tag{7}$$

Dynamics of surfactant adsorption:

$$\theta_s(t') = c_b\frac{\sqrt{\mathcal{D}}}{\Gamma_m}\frac{1}{\sqrt{\pi}}\left[2\sqrt{t'} - \int_0^{t'} \frac{C_s'(\tau')}{\sqrt{t'-\tau'}}\mathrm{d}\tau'\right] \tag{8}$$

Adsorption isotherm of surfactant:

$$C_s'(t') = \frac{\theta_s(t')}{\kappa_s\left[1-\theta_p(t')-\theta_s(t')\right]}\exp\left[-2\alpha_s\theta_s(t') - 2\alpha_{ps}\theta_p(t')\right] \tag{9}$$

And the equation of state:

$$\Pi' = -\ln(1-\theta_p-\theta_s) - \theta_p(1-\omega_0/\omega_p) - \alpha_p\theta_p^2 - \alpha_s\theta_s^2 - 2\alpha_{ps}\theta_p\theta_s \tag{10}$$

where $\Pi' = \Pi\omega_0/(RT)$ is the dimensionless surface pressure, $\theta_p = \Gamma_p/\Gamma_{pm}$ is the dimensionless surface concentration of protein (i.e. the coverage fraction), $\theta_s = \Gamma_s/\Gamma_{sm}$ is the dimensionless surface concentration (coverage fraction) of surfactant, $\Gamma_{pm} = 1/\omega_p$ and $\Gamma_{sm} = 1/\omega_s$ are the maximum surface concentration of protein and surfactant respectively (both measures of surface capacity), $t' = (D_p\, t)/(\Gamma_{pm}/C_{pb})^2$ is the dimensionless time, $C_p' = C_p/C_{pb}$ is the dimensionless bulk concentration of protein at the layer next to the surface, $C_s' = C_s/C_{sb}$ is the dimensionless bulk concentration of surfactant at the layer next to the surface, C_{pb} and C_{sb} are the initial bulk concentration of protein and surfactant respectively, $\kappa_p = b_pC_{pb}$ and $\kappa_s = b_sC_{sb}$ are the dimensionless adsorption equilibrium constant of protein and surfactant, respectively (both measures of surface affinity), $c_b = C_{sb}/C_{pb}$ is the relative bulk concentration, $\mathcal{D} = D_s/D_p$ is the relative diffusivity and $\Gamma_m = \Gamma_{sm}/\Gamma_{pm} = \omega_p/\omega_s$ is the relative capacity which is equivalent to the ratio between molar areas of protein and surfactant.

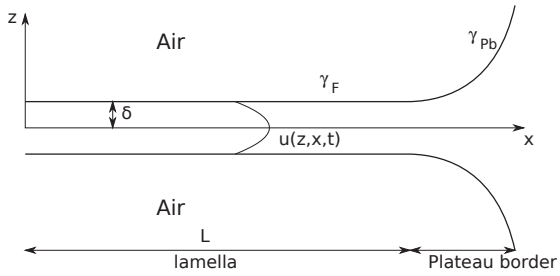

Fig. 1: Two-dimensional slice of a lamella

III. Surfactant transport onto a foam lamella

As the surface active material is adsorbed from the bulk liquid onto the surface of the Plateau border and the film, the gradient of concentration between the Plateau border and the foam film leads to a gradient of surface tension. When there is gradient of surface tension, the Marangoni effect takes place, causing the Marangoni flow from the region with low surface tension to the region with higher surface tension. For systems of interest here, the direction of the Marangoni flow is towards the centre of the film, opposite to the direction of the film drainage. This Marangoni effect is important for transport of surface active material from the surface of Plateau borders onto the surface of foam lamellae. Moreover, the Marangoni effect contributes to the stabilisation of the liquid film [11], [27] as its direction is opposite to the film drainage, therefore reduces the surface mobility. Therefore this transport plays an important role in determination of the efficiency of a foam fractionation column.

A schematic diagram of a two-dimensional slice through a lamella is shown in Fig. 1. In this study, the interfaces between the liquid film and the air bubble are assumed to be symmetric [22]. At the Plateau border, the curvature of the gas-liquid interface causes lower pressure in the liquid. As a consequence, there is a suction of liquid from the lamella to the Plateau border [22]. The surface concentration of surfactant on the Plateau border interface is higher than the surface concentration of liquid on the lamella interface due to the enrichment of surfactant concentration from the reflux stream. Therefore, the interface at the Plateau border has a lower surface tension than the interface on the lamella. Because of that gradient of surface tension, there is a Marangoni flow on the surface from the low surface tension to the higher surface tension.

The equation for the profile of surface velocity taking into account the surface viscosity is developed based on the lubrication theory. The profile of the surface velocity can be expressed by the following equation:

$$u_s = -\frac{x}{\delta}\frac{\mathrm{d}\delta}{\mathrm{d}t} + \frac{\delta}{3\mu}\left[\frac{\partial\gamma}{\partial x} + \frac{\partial}{\partial x}\left(\mu_s\frac{\partial u_s}{\partial x}\right)\right] \tag{11}$$

where $u_s = \mathrm{d}x/\mathrm{d}t$ is the surface velocity, x is the distance from the centre of the lamella along the x axis, t is time, δ is the half thickness of the lamella, μ is the liquid viscosity, γ is the surface tension, μ_s is the surface viscosity. Applying the Gibbs equilibrium [37] to the surface tension to convert it into surface excess of surfactant results in the following equation:

$$\frac{3\mu}{\delta}\left(u_s + \frac{x}{\delta}\frac{\mathrm{d}\delta}{\mathrm{d}t}\right) = \frac{\partial}{\partial x}\left(-G\ln\frac{\Gamma}{\Gamma_{Pb}}\right) + \frac{\partial}{\partial x}\left(\mu_s\frac{\partial u_s}{\partial x}\right) \tag{12}$$

where G is the Gibbs parameter, Γ is the surface excess of surfactant on the surface of the film and Γ_{Pb} is the surface excess of surfactant on the surface of the Plateau border. This is generally larger than the surface excess on the film (Γ or Γ_{F0} initially at time $t = 0$).

The foregoing analysis has concerned itself with determining simple (albeit plausible) fluid flow fields for a foam film. We now adopt an approach similar to that of [38], i.e. we use those flow fields within a mass balance equation. Specifically a surfactant mass balance using the assumption of insoluble surfactant is developed. Using this assumption, the surfactant stays on the interface once it is adsorbed. Therefore, there is no surfactant present within the bulk of film (i.e. surfactant diffusion is ignored). The surfactant mass balance for insoluble surfactant is presented as follows:

$$\frac{\partial\Gamma}{\partial t} + \frac{\partial}{\partial x}(u_s\Gamma) = 0. \tag{13}$$

Knowledge of the film thinning rate $\mathrm{d}\delta/\mathrm{d}t$ is required to solve Eq. (12). Note however that $\mathrm{d}\delta/\mathrm{d}t$ is a parameter that we must input to this (uniform film thickness) model – it is not something we can predict within the framework of our model – without describing how the film interacts with Plateau borders around its edges (possibly considering also complex phenomena e.g. dimpling, non-uniformities of the film, as mentioned previously). Evolution of film thickness and hence $\mathrm{d}\delta/\mathrm{d}t$ can however in principle be measured experimentally via a device such as Scheludko cell [39], [40], [41] so an empirical $\mathrm{d}\delta/\mathrm{d}t$ formula could be obtained, even in the absence of a detailed model. Alternatively we could employ theoretical estimates of the thinning rate sourced from literature.

In what follows two approaches to estimating this thinning rate are discussed. One approach is based on the assumption of a mobile interface, while the other approach is based on the assumption of a rigid surface, using the so called Reynolds equation.

The rate of film thinning for a film with a mobile interface is determined based on the studies by [22] and [23] (see also [26]). In this study, half of the film thickness δ is used as the dependent variable instead of the full thickness, for determination of the following equation:

$$\frac{\mathrm{d}\delta}{\mathrm{d}t} = -\frac{3}{8}\frac{\gamma_{Pb}\delta^{3/2}}{\mu L\sqrt{a}}. \tag{14}$$

When the film has rigid interfaces, the drainage follows the theory developed by [42] (see also [43], [44]). The thinning rate is determined by application of the lubrication approximation to the Navier-Stokes equation resulting in the Reynolds equation as follows:

$$\frac{\mathrm{d}\delta}{\mathrm{d}t} = -\frac{\delta^3\Delta P}{3\mu L^2} \tag{15}$$

where ΔP is the excess pressure in the foam film as the driving force of the film drainage and can be expressed as $\Delta P = P_c - \Pi$, where P_c is the capillary pressure and Π is the disjoining pressure [45].

A dimensional analysis was carried out upon Eq. (12) and results in the following equation:

$$\frac{3}{\delta'}\left(u_s' + \frac{x'}{\delta'}\frac{\mathrm{d}\delta'}{\mathrm{d}t'}\right) = -\frac{1}{\delta_0'}\frac{\partial\ln\Gamma'}{\partial x'} + \frac{\partial}{\partial x'}\left(\bar{\mu}_s\frac{\partial u_s'}{\partial x'}\right) \tag{16}$$

where $u_s' = u_s\mu/G\delta_0'$ is the dimensionless surface velocity, $\delta_0' = \delta_0/L$ is the dimensionless initial half film thickness, δ_0 is the initial half film thickness, L is half of the film length, $\delta' = \delta/L$ is the dimensionless half film thickness, $x' = x/L$ is the dimensionless distance from the centre of the lamella along the x axis, $t' = tG\delta_0'/L\mu$ is the dimensionless time, $\Gamma' = \Gamma/\Gamma_{Pb}$ is the dimensionless surface excess of surfactant and $\bar{\mu}_s = \mu_s/\mu L$ is the dimensionless surface viscosity. The dimensionless surface viscosity is the reciprocal of the surface mobility parameter identified by Leonard and Lemlich in their study [21], [46].

The dimensionless form of the thinning equation for a film with a mobile interface is as follows:

$$\frac{\mathrm{d}\delta'}{\mathrm{d}t'} = -\frac{3}{8}\frac{\delta'^{3/2}}{\delta_0'\bar{G}\sqrt{a'}}. \tag{17}$$

and the dimensionless form of the thinning equation for a film with a mobile interface is as follows:

$$\frac{\mathrm{d}\delta'}{\mathrm{d}t'} = -\frac{\delta'^3}{3\delta_0'\bar{G}\,a'}. \tag{18}$$

IV. Parameter values

A. Mixed protein-surfactant adsorption

The parameters used in the simulation are obtained from a study by Miller et al. [19] using Bovine β-lactoglobulin (BLG) protein and nonionic decyl dimethyl phosphine oxide (C_{10}DMPO) surfactant. Those parameters are listed in Table I. The parameters from the study by Miller et al. were set as a base case when the simulation involved variation of the material parameters such as diffusion constant of surfactant D_s (or analogously $\mathcal{D}$ in dimensionless form), surface capacity of surfactant Γ_{sm} (or analogously dimensionless Γ_m), adsorption coefficient of surfactant, b_s (or analogously κ_s) and adsorption coefficient of protein, b_p (or analogously κ_p).

B. Surfactant transport

The present work performs a simulation study of the effect of surface viscosity on the transport of bovine serum albumin (BSA) together with a cosurfactant propylene glycol alginate (PGA) onto a foam film during a process of foam fractionation. Typical parameters values for the simulation are presented in

TABLE I: The values of base case parameters used in the simulation of adsorption dynamics.

Parameter	Value	Unit
D_p	5×10^{-11}	$\mathrm{m^2\,s^{-1}}$
D_s	4×10^{-10}	$\mathrm{m^2\,s^{-1}}$
C_{pb}	1×10^{-3}	$\mathrm{mol\,m^{-3}}$
C_{sb}	1×10^{-2}	$\mathrm{mol\,m^{-3}}$
R	8.3144621	$\mathrm{J\,mol^{-1}\,K^{-1}}$
T	298	K
ω_0	3.5×10^5	$\mathrm{m^2\,mol^{-1}}$
ω_p	4.4×10^6	$\mathrm{m^2\,mol^{-1}}$
ω_s	2.5×10^5	$\mathrm{m^2\,mol^{-1}}$
Γ_{pm}	2.27×10^{-7}	$\mathrm{mol\,m^{-2}}$
Γ_{sm}	4.00×10^{-6}	$\mathrm{mol\,m^{-2}}$
α_p	0.4	
α_s	-0.25	
α_{ps}	0.075	
b_p	1.4×10^3	$\mathrm{m^3\,mol^{-1}}$
b_s	21.9	$\mathrm{m^3\,mol^{-1}}$

TABLE II: Parameters for simulation of surfactant transport onto a foam lamella.

Parameters	Value	Unit
δ_0	20×10^{-6}	m
δ_{cb}	15×10^{-9}	m
L	5×10^{-3}	m
μ	7×10^{-3}	Pa s
μ_s	$31 \pm 12 \times 10^{-3}$	Pa m s
Γ_{Pb}	3×10^{-8}	$\mathrm{mol\,m^{-2}}$
Γ_{F0}	1.5×10^{-8}	$\mathrm{mol\,m^{-2}}$
a	5×10^{-4}	m
γ_{Pb}	55×10^{-3}	$\mathrm{N\,m^{-1}}$
G	$65 \pm 12 \times 10^{-3}$	$\mathrm{N\,m^{-1}}$

Tab. II. All parameters except the values of Γ_{Pb}, Γ_{F0}, δ_{cb}, δ_0' and a were taken from the study by Durand and Stone [37] using protein BSA together with a cosurfactant PGA, both at concentration of $4.0\,\mathrm{g\,L^{-1}}$. The value of a was estimated as presented in the work by Vitasari et al. [47], while the value of δ_{cb} was taken from Weaire and Hutzler [8]. The values of Γ_{Pb}, Γ_{F0} are estimates, taken as lower than the maximum surface excess Γ_{max} of BSA which was reported in a study by Fainerman et al. which is $\Gamma_{max} = 5 \times 10^{-8}$ [33]. Those parameters are base-case parameters and variations about the base-case will be applied in the simulations.

V. Results and Discussion

A. Competition between protein and surfactant molecules on the surface

Figure 2, corresponding to the base case parameter values, shows the comparison between the dimensionless subsurface concentration of protein and the dimensionless subsurface concentration of surfactant at base case. This simulation was carried out using these values of dimensionless groups: $\kappa_p = 1.4$, $\kappa_s = 0.219$, $\mathcal{D} = 8$, $\Gamma_m = 17.6$, $c_b = 10$. Since the diffusivity coefficient of surfactant is higher than the diffusivity coefficient of protein, surfactant is more rapidly transferred to the subsurface. At early time, there is therefore more surfactant adsorbed on the surface. Due to the faster diffusion (high

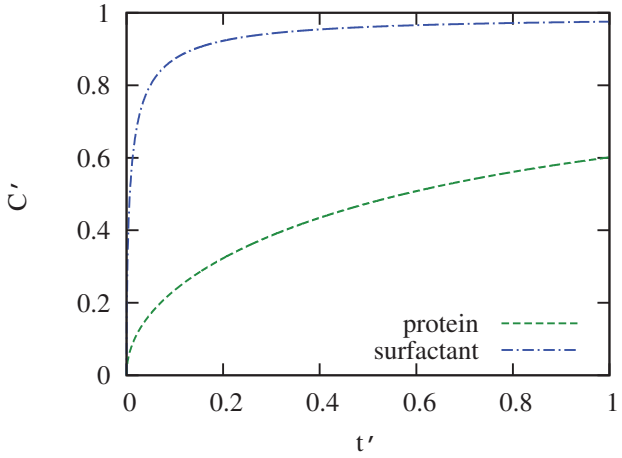

Fig. 2: Dimensionless subsurface concentration as a function of dimensionless time observed at dimensionless parameters of: $\kappa_p = 1.4$, $\kappa_s = 0.219$, $\mathcal{D} = 8$, $\Gamma_m = 17.6$, $c_b = 10$.

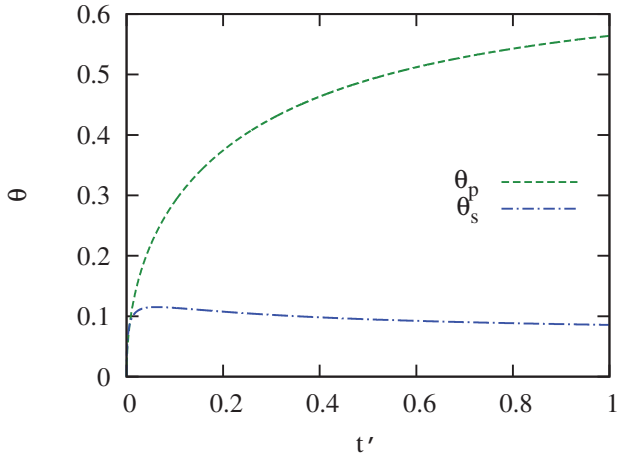

Fig. 3: Surface coverage as a function of dimensionless time observed at dimensionless parameters of: $\kappa_p = 1.4$, $\kappa_s = 0.219$, $\mathcal{D} = 8$, $\Gamma_m = 17.6$, $c_b = 10$.

$\mathcal{D}$), and also lower surface affinity (viz. the low value of the parameter κ_s), surfactant reaches its final concentration in the subsurface faster than protein. The subsequent arrival of additional protein in the subsurface provides more protein molecules to adsorb to the interface while there is limited further change of surfactant concentration in the subsurface. As protein has a relatively higher surface affinity (measured by the values of κ_p vs. κ_s), protein molecules compete strongly with surfactant molecules on the surface. Therefore, protein molecules replace surfactant molecules on the surface resulting in lower surface concentration of surfactant as presented in Figure 3. This overshoot phenomenon also occurs in the adsorption of mixed surfactants as reported by Mulqueen et al. [48].

Figure 4 shows the growth of the surface pressure with the addition of protein in the bulk solution where the values of the dimensionless groups are: $\kappa_p = 1.4$, $\kappa_s = 0.219$, $\mathcal{D} = 8$, $\Gamma_m = 17.6$, $c_b = 10$. The time scale of this figure is taken up to five units, longer than the time scale of Figures 2 and 3 which is up to one unit. The longer time scale in Figure 4 has been selected to show the final surface pressure is approached on that time scale. The surface pressure is higher in the presence of protein and surfactant in the bulk solution compared to the surface pressure resulting from pure surfactant or pure protein solution. For a fixed amount of surfactant on the surface (dashed-dotted line), which was set to be the final surface concentration of surfactant in the presence of protein ($\theta_s = 0.0728$), in general, lower surface pressure occurs compared to that obtained from simulation of dynamic concentrations of protein and surfactant on the surface. This happens since the fixed surfactant surface concentration is mostly lower than the dynamic surface concentration, the only exceptions being at very early times and at the final time. Although difficult to resolve on the scale of the graph, at very early time, the surface pressure is higher in the case of fixed surface coverage of surfactant due to finite surfactant concentration on the surface initially. By contrast, in the dynamic case, the surface concentration of surfactant has to grow from zero at very early times. At final time, of course the surface pressure of those both cases will be equal since by that time the dynamic surface concentration of surfactant reaches its final value that is equal to the selected fixed surface concentration. The graph also indicates that protein concentration on the surface is able to increase (and thereby influence surface pressure) even with the presence of significant surfactant on the surface. Protein with its higher affinity is able to compete with surfactant to adsorb on the surface.

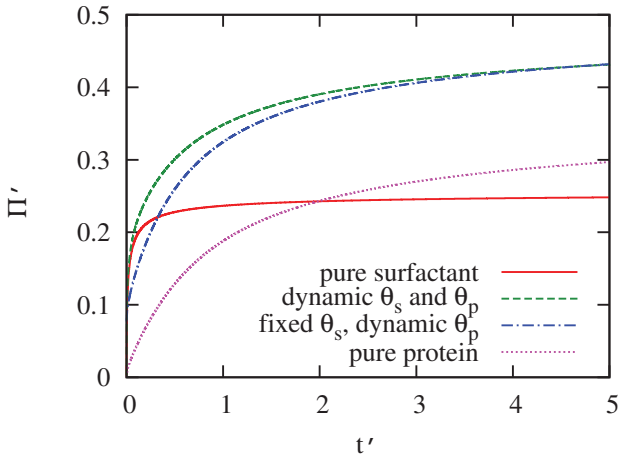

Fig. 4: Dimensionless surface pressure as a function of dimensionless time at various protein-surfactant composition using dimensionless parameters of: $\kappa_p = 1.4$, $\kappa_s = 0.219$, $\mathcal{D} = 8$, $\Gamma_m = 17.6$, $c_b = 10$ (solid line: pure surfactant; dashed line: dynamic protein and dynamic surfactant surface concentration; dotted line: dynamic protein and fixed surfactant surface concentration; dashed-dotted line: pure protein.

B. Numerical simulation of surfactant transport in the case with film drainage

In this simulation, there are, as we have stated, two approaches to predict the rate of film drainage. One uses an assumption of a mobile film surface, and the other uses the assumption of a rigid film surface. Therefore, some notion of the degree of surface mobility needs to be available in order to select the appropriate film drainage equation. The choice of surfactant determines the surface mobility as studied by [49],

The predicted drainage rate of film with a mobile interface is very fast. Without any evaporation, film thinning is limited to a final film thickness of the order of 30 nm ($\delta_{\text{cut-off}} = 15\,\text{nm}$) to form a film known as a common black film [50]. The film does not thin further due to electrostatic repulsion within it [51], [50], [52]. In this simulation with a mobile interface, the film reaches the thickness of common black film at $t' = 3.6$, corresponding to dimensional time $t = 0.1\,\text{s}$, which is much shorter than the residence time in the foam fractionation column at $t' = 383$, which corresponds to dimensional time about $t = 12\,\text{s}$. After reaching the thickness of common black film, the lamella does not thin further due to electrostatic repulsion between the layers (assuming of course sufficient surfactant still remains to stabilise the film). We incorporate this repulsion in an approximate fashion as a sharp cut-off of the thinning rate at a specified δ' taken as 3×10^{-6}, although in reality the decay of the drainage rate would be spread over a range of δ' values: one could model that comparatively easily via so called double layer theory, with an electrostatic disjoining pressure which would start to grow as soon as film thickness fell to within a few Debye lengths [53] of the cut-off thickness (since the electrostatic interaction between surfaces or particles has an exponential behaviour with a characteristic length equal to the Debye length [54]), and which would exactly balance the Plateau border capillary suction pressure precisely when that cut-off thickness was achieved. The predicted thinning of a film with a mobile interface is presented in Fig. 5. The time scale is taken to $t' = 400$, close to the residence time inside a foam fractionation column.

On the other hand, a film with a rigid interface drains orders of magnitudes slower than one with a mobile interface. Reaching $\delta_{\text{cut-off}}$ takes dimensionless time $t' = 5.93 \times 10^7$ which corresponds to $t = 1.85 \times 10^6\,\text{s}$. Therefore, the film with a rigid interface will not reach the thickness of common black film during the residence time in the foam fractionation column. The thinning of film with a rigid interface is presented in Fig. 6. Note that, even though the film fails to approach anything near a common black film within the residence time available, significant thinning does in fact take place. It is a poor approximation to treat the film as having a fixed thickness.

The choice of film thinning rate equation, impacts on the surfactant concentration. When the assumption of a mobile interface is utilised, the film thinning rate follows the equation

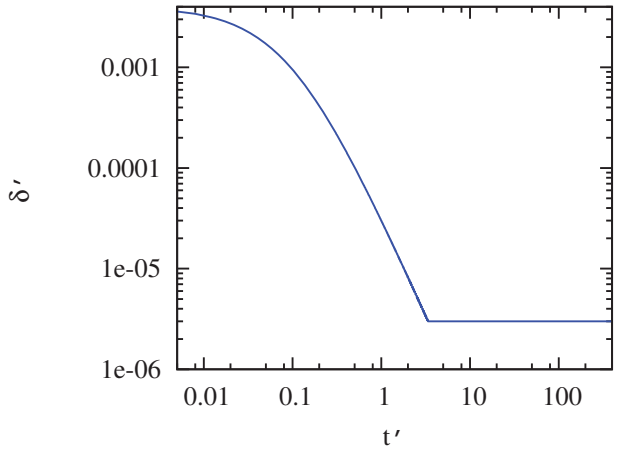

Fig. 5: Change of dimensionless film thickness δ' with dimensionless time t' in the case of a mobile interface.

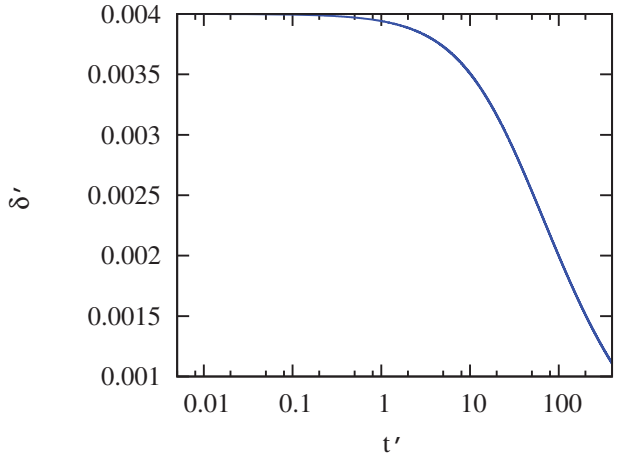

Fig. 6: Change of dimensionless film thickness δ' with dimensionless time t' in the case of a rigid interface.

developed by [22]. The result of the consequent simulation for Γ' is presented in Fig. 7. In this simulation, drainage is driving liquid rapidly out of the film. On the surface, however there can be a Marangoni force that causes the liquid to flow in the direction away from the Plateau border. If the Marangoni flow were to dominate the film drainage, surfactant would accumulate on the surface. However, in this simulation, the film drainage (initially) dominates the Marangoni flow. Therefore, surfactant will be washed away from the surface. As surfactant is washed away, the surface concentration of surfactant on the film surface becomes lower. According to the model predictions, Marangoni stresses are unimportant away from the film edges, but near the film edges they might retain importance.

The film drains and thins however only until it reaches the thickness of a common black film. At this thickness, there is

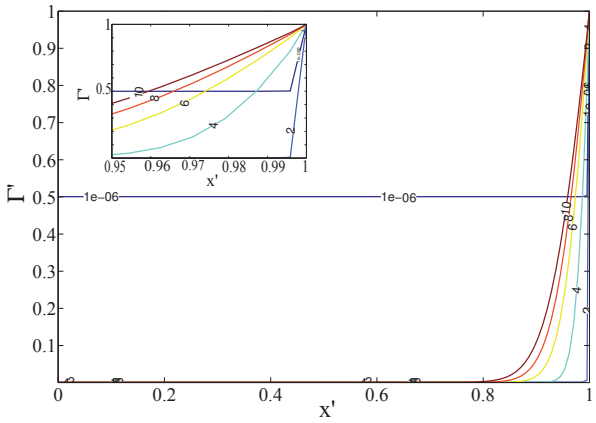

Fig. 7: Evolution predicted for dimensionless surfactant surface concentration Γ' along the film length x' with film drainage using the assumption of a mobile interface. Labels on the lines represent the dimensionless time t'. The inset is zoomed in within the spatial range 0.95 to 1 spatial unit.

no further thinning, therefore only the Marangoni effect takes place thereafter and this determines the subsequent surfactant transport. As a result, surfactant begins to accumulate on the film surface again, albeit starting from a rather low concentration level. However, since the film is very thin, the Marangoni effect is weak and the surfactant accumulation is much slower than that which occurs on a substantially thicker film such as in the case without film drainage. Remember however that here we switch off the film drainage abruptly at a certain cut-off thickness. Were we to reduce the rate of film drainage rate more gradually (by allowing a film disjoining pressure to build up with falling film thickness) then we could potentially begin transferring surfactant back onto the film at a slightly larger thickness, where the mass transfer rate would be likewise slightly larger.

The following simulation result presented in Fig. 8 is based on the assumption of a rigid interface. The thinning rate of the film then follows the Reynolds equation. Comparing Eq. (17) with Eq. (18), the thinning rate determined using the assumption of a rigid interface is much slower than the thinning rate using the assumption of a mobile interface. As a consequence, the Marangoni flow dominates the film drainage, therefore, surfactant accumulates on the film surface right from the beginning. At any given time however there is less surfactant on the surface than there would have been in the absence of film drainage.

One of the interesting results to obtain from the simulation of surfactant transport onto a foam lamella is the net accumulation of surfactant on the film surface with time. Fig. 9 presents the spatially-averaged surfactant concentration on the film surface $\langle\Gamma'\rangle$ with time t' for films without drainage, and for a draining film with a mobile interface and that with a rigid interface. In the case of a film without drainage and

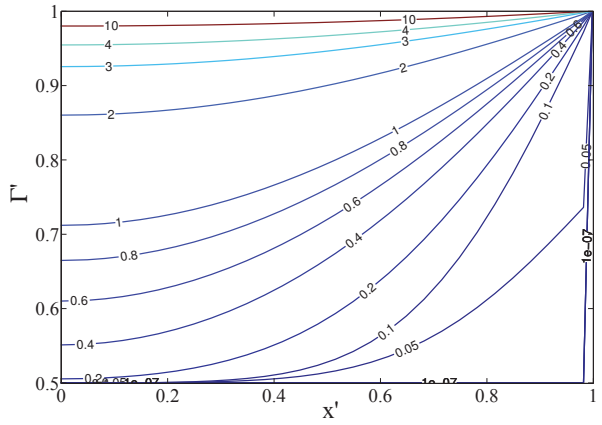

Fig. 8: Evolution of dimensionless surfactant surface concentration Γ' along the film length x' with film drainage using the assumption of a rigid interface. Labels on the lines represent the dimensionless time t'.

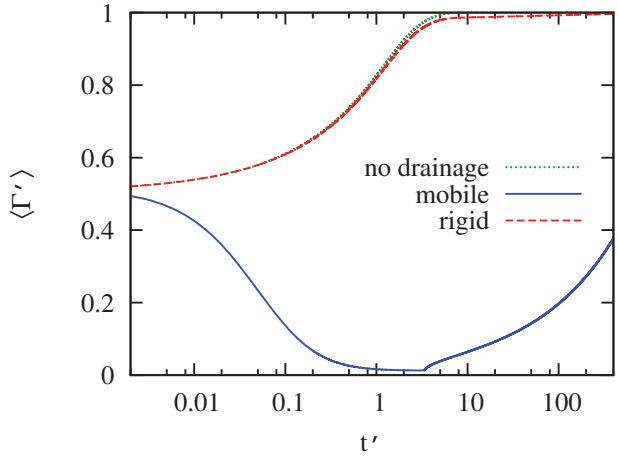

Fig. 9: Predictions for spatially averaged dimensionless surfactant surface concentration $\langle\Gamma'\rangle$ vs dimensionless time t' on the surface of films with in the case of no film drainage as well as with drainage assuming films with a mobile and with a rigid interface.

a draining film with a rigid interface, since the Marangoni effect dominates, the amount of surfactant on the film surface increases with time and reaches a final equilibrium at a much shorter time than the residence time in the foam column. On the other hand, the amount of surfactant on the surface of the film with a mobile interface decreases with time until a particular time and subsequently increases with time due to the absence of any further film drainage. With a mobile interface, as long as the thickness of film is above the thickness of a common black film, the drainage is very fast and dominates the Marangoni effect. As a consequence, the concentration of surfactant on the film surface decreases with time (although in reality the decrease is unlikely to be anywhere near as dramatic as Fig. 9 suggests, because Marangoni stresses will feed back to the film thinning rate, reducing the rate at which surfactant can be washed off the film). The subsequent increase of the amount of surfactant on the surface of film with a mobile interface only occurs when there is no further film drainage once the film is as thin as a common black film. Since the film is very thin, the Marangoni effect is however weak, and the accumulation of surfactant is quite slow.

C. Surfactant transport onto a foam lamella in the presence of surface viscosity

The profile of surface velocity obtained from simulation for this case is presented in Fig. 10.

At early time, the magnitude of u'_s (away from $x' = 1$) grows. As the width of the region near $x' = 1$ over which the system deviates from uniform Γ' grows, the magnitude of $\partial u''_s/\partial x'$ outside this region also grows. At later times however, the magnitude of $\partial u''_s/\partial x'$ decays due to the gradients of surface concentration eventually decaying as more and more surfactant accumulates on the film surface. The magnitude of surface velocity at the end of the film is a decreasing function of time as shown by the inset in Fig. 10. The subsequent decay

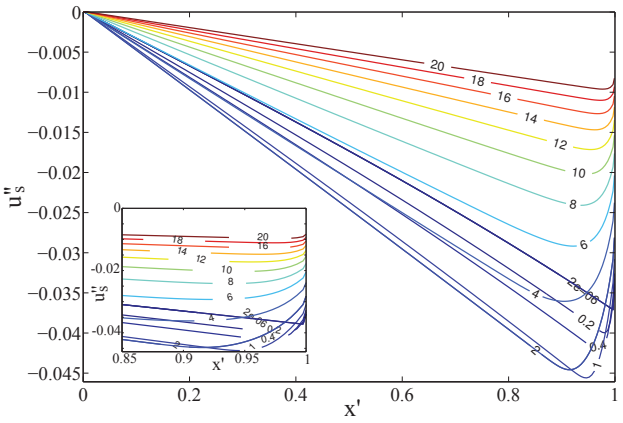

Fig. 10: Evolution of surface velocity in the absence of film drainage calculated using $\delta'_0\bar{\mu}_s = 5.4$ (obtained from $\delta'_0 = 6 \times 10^{-5}$ and $\bar{\mu}_s = 8.86 \times 10^4$), $a' = 0.1$ and $\Gamma'_{F0} = 0.5$. The computation was carried out using the finite difference method. Labels on curves are the rescaled dimensionless time t''. The inset is zoomed in around $x' = 1$. The velocity profiles show a linear variation with x' over much of the domain, but an abrupt deviation from linearity near $x' = 1$.

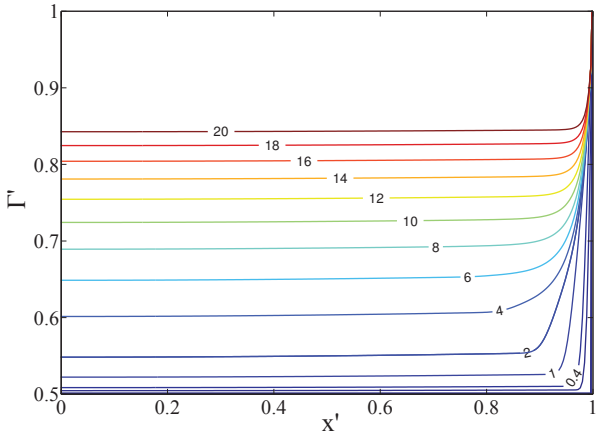

Fig. 11: Evolution of surfactant surface concentration in the absence of film drainage calculated using parameters $\delta_0'\bar{\mu}_s = 5.4$ (obtained from $\delta_0' = 6 \times 10^{-5}$ and $\bar{\mu}_s = 8.86 \times 10^4$), $a' = 0.1$ and $\Gamma'_{F0} = 0.5$. The computation was carried out using the finite difference method. Labels on curves are the rescaled dimensionless time t''. The profiles show a uniform concentration region over much of the domain with an abrupt change in concentration at the end of the domain.

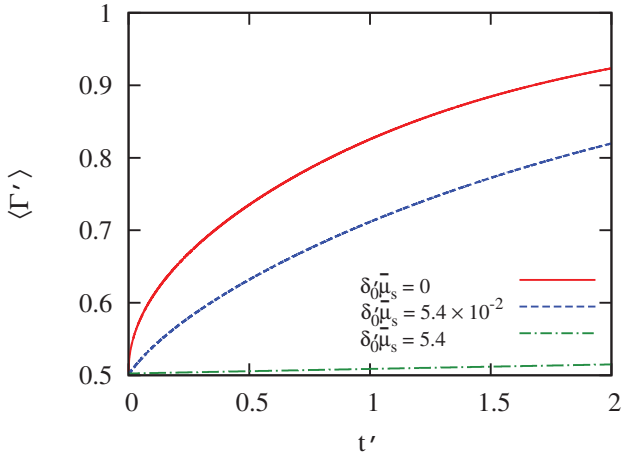

Fig. 12: Comparison of the average surfactant surface concentration over time calculated in the absence of surface viscosity and in the presence of surface viscosity ($\delta_0'\bar{\mu}_s = 0 - 5.4$, $\bar{\mu}_s = 0 - 8.86 \times 10^4$). The simulation was using $\delta_0' = 6 \times 10^{-5}$, $a' = 0.1$ and $\Gamma'_{F0} = 0.5$. The computation was carried out using the finite difference method. High surface viscosity severely limits the rate at which surfactant accumulates on the film.

in the velocity is due to the gradient of surface concentration at $x' = 1$ reducing with time due to transport of surfactant onto the lamella.

The profile of surfactant surface concentration is calculated using the material point method based on the calculated surface velocity presented in Fig. 10. The profile of surfactant surface concentration is presented in Fig. 11.

At positions far from the Plateau border, the surface velocity is proportional to the distance from the centre of the film. Near the Plateau border, the surface velocity profile turns around to satisfy the boundary condition at $x' = 1$. Moreover, the surface concentration of surfactant is uniformly distributed along the film except at positions near the Plateau border. Interestingly, we never seem to achieve a state which the spatial variation of Γ' is spread over the entire film.

The spatially averaged surfactant surface concentration at any given time for the case of large surface viscosity has been calculated and the result is rescaled to match the case of small surface viscosity. The result is presented in Fig. 12. The rate of surfactant transport onto the lamella surface is much slower with large surface viscosity parameter compared with that for a small surface viscosity parameter and that without surface viscosity. The larger surface viscosity results in larger surface viscous effect that opposes the Marangoni effect. As a result, the magnitude of surface velocity is much smaller, result in less surfactant transported onto the surface of the lamella.

VI. Conclusion

The adsorption behaviour of mixed protein-surfactant is different from that of single surfactant, where there is competition between protein and surfactant molecules to occupy the interface. The Frumkin isotherm represents the equilibrium of adsorption on the bubble surface. The diffusion of protein is slower than that of surfactant. However, the protein will displace surfactant once it reaches the interface due to the higher surface affinity of protein. However, there is a critical affinity of protein for displacement of surfactant to occur. This critical affinity need not necessarily be higher than the affinity of surfactant. However, the displacement is more likely to occur when the affinity of protein is much higher and the diffusivity of protein is lower than those of surfactant.

The film drainage modelled using a mobile interface is much faster than that modelled using assumption of a rigid interface. The film drainage dominates the Marangoni flow in the case of a lamella with a mobile interface, therefore surfactant is washed away from the surface of the foam lamella. Having a mobile interface, a film possibly achieves the thickness of a common black film, when the drainage stops to occur, during the residence time in a foam fractionation column with reflux. In the absence of film drainage, at the thickness of common black film, surfactant will accumulate on the surface of the lamella. The desirable condition for operation of a foam fractionation column is when the Marangoni flow dominates the film drainage which can be achieved by employing surfactant that gives a rigid interface.

The surface viscous effect reduces the amount of surfactant transport and a larger the surface viscosity results in less surfactant transport onto a foam lamella. For a large surface viscosity, not only the surfactant transport is slow, but also the profile of surface velocity is proportional to the distance from

the centre of a lamella, resulting in nearly uniform distribution of surfactant surface coverage, except within a boundary layer near the Plateau border.

ACKNOWLEDGMENT

D. Vitasari would like to give thanks for funding support to carry out this PhD study provided by Directorate General of Higher Education Republic of Indonesia.

REFERENCES

[1] A. P. Shea, C. L. Crofcheck, F. A. Payne, and Y. L. Xiong, "Foam fractionation of α-lactalbumin and β-lactoglobulin from a whey solution," *Asia-Pacific Journal of Chemical Engineering*, vol. 4, no. 2, pp. 191–203, 2009.

[2] B. M. Gerken, A. Nicolai, D. Linke, H. Zorn, R. G. Berger, and H. Parlar, "Effective enrichment and recovery of laccase C using continuous foam fractionation," *Separation and Purification Technology*, vol. 49, no. 3, pp. 291–294, 2006.

[3] V. Burapatana, A. Prokop, and R. D. Tanner, "Enhancing cellulase foam fractionation with addition of surfactant," *Applied Biochemistry and Biotechnology*, vol. 122, no. 1-3, pp. 541–552, 2005.

[4] B. Burghoff, "Foam fractionation applications," *Journal of Biotechnology*, vol. 161, no. 2, pp. 126–137, 2012.

[5] V. Burapatana, E. A. Booth, I. M. Snyder, A. Prokop, and R. D. Tanner, "A proposed mechanism for detergent-assisted foam fractionation of lysozyme and cellulase restored with β-cyclodextrin," in *Applied Biochemistry and Biotecnology* (J. R. Mielenz, K. T. Klasson, W. S. Adney, and J. D. McMillan, eds.), ABAB Symposium, pp. 777–791, Humana Press, 2007.

[6] R. Lemlich, "Adsorptive bubble separation methods: Foam fractionation and allied techniques," *Industrial and Engineering Chemistry*, vol. 60, no. 10, pp. 16–29, 1968.

[7] P. Stevenson, *Foam Engineering: Fundamentals and Applications*. Wiley, 2012.

[8] D. Weaire and S. Hutzler, *The Physics of Foams*. Oxford University Press, New York, 1999.

[9] J. Maldonado-Valderrama and D. Langevin, "On the difference between foams stabilized by surfactants and whole casein or β-casein. comparison of foams, foam films, and liquid surfaces studies," *The Journal of Physical Chemistry B*, vol. 112, no. 13, pp. 3989–3996, 2008.

[10] S. Boonyasuwat, S. Chavadej, P. Malakul, and J. F. Scamehorn, "Anionic and cationic surfactant recovery from water using a multistage foam fractionator," *Chemical Engineering Journal*, vol. 93, no. 3, pp. 241–252, 2003.

[11] L. Y. Yeo, O. K. Matar, E. P. de Ortiz, and G. F. Hewitt, "Film drainage between two surfactant-coated drops colliding at constant approach velocity," *Journal of Colloid and Interface Science*, vol. 257, pp. 93–107, 2003.

[12] B. P. Radoëv, D. S. Dimitrov, and I. B. Ivanov, "Hydrodynamics of thin liquid films effect of the surfactant on the rate of thinning," *Colloid and Polymer Science*, vol. 252, no. 1, pp. 50–55, 1974.

[13] T. T. Traykov and I. B. Ivanov, "Hydrodynamics of thin liquid films. effect of surfactants on the velocity of thinning of emulsion films," *International Journal of Multiphase Flow*, vol. 3, no. 5, pp. 471–483, 1977.

[14] A. Mackie and P. Wilde, "The role of interactions in defining the structure of mixed protein-surfactant interfaces," *Advances in Colloid and Interface Science*, vol. 117, pp. 3–13, 2005.

[15] J. Maldonado-Valderrama and J. M. R. Patino, "Interfacial rheology of protein-surfactant mixtures," *Current Opinion in Colloid & Interface Science*, vol. 15, no. 4, pp. 271–282, 2010.

[16] R. Miller, V. Fainerman, A. Makievski, J. Krägel, and R. Wüstneck, "Adsorption characteristics of mixed monolayers of a globular protein and a non-ionic surfactant," *Colloids and Surfaces A: Physicochemical and Engineering Aspects*, vol. 161, no. 1, pp. 151 – 157, 2000.

[17] E. Dickinson, "Adsorbed protein layers at fluid interfaces: Interactions, structure and surface rheology," *Colloids and Surfaces B: Biointerfaces*, vol. 15, no. 2, pp. 161–176, 1999.

[18] J. Krägel, R. Wüstneck, F. Husband, P. J. Wilde, A. V. Makievski, D. O. Grigoriev, and J. B. Li, "Properties of mixed protein/surfactant adsorption layers," *Colloids and Surfaces B: Biointerfaces*, vol. 12, no. 3-6, pp. 399–407, 1999.

[19] R. Miller, V. B. Fainerman, M. E. Leser, and M. Michel, "Kinetics of adsorption of proteins and surfactants," *Current Opinion in Colloid & Interface Science*, vol. 9, no. 5, pp. 350 – 356, 2004.

[20] L. N. Brush and S. H. Davis, "A new law of thinning in foam dynamics," *Journal of Fluid Mechanics*, vol. 534, pp. 227–236, 2005.

[21] R. A. Leonard and R. Lemlich, "A study of interstitial liquid flow in foam. Part I. Theoretical model and application to foam fractionation," *AIChE J.*, vol. 11, no. 1, pp. 18–25, 1965.

[22] C. J. W. Breward and P. D. Howell, "The drainage of a foam lamella," *Journal of Fluid Mechanics*, vol. 458, pp. 379–406, 2002.

[23] P. S. Stewart and S. H. Davis, "Dynamics and stability of metallic foams: Network modeling," *Journal of Rheology*, vol. 56, no. 3, pp. 543–574, 2012.

[24] P. J. Martin, H. M. Dutton, J. B. Winterburn, S. Baker, and A. B. Russell, "Foam fractionation with reflux," *Chemical Engineering Science*, vol. 65, no. 12, pp. 3825 – 3835, 2010.

[25] P. Stevenson and G. J. Jameson, "Modelling continuous foam fractionation with reflux," *Chemical Engineering and Processing: Process Intensification*, vol. 46, no. 12, pp. 1286–1291, 2007.

[26] P. S. Stewart and S. H. Davis, "Self-similar coalescence of clean foams," *Journal of Fluid Mechanics*, vol. 722, pp. 645–664, 2013.

[27] S. I. Karakashev and A. V. Nguyen, "Effect of sodium dodecyl sulphate and dodecanol mixtures on foam film drainage: Examining influence of surface rheology and intermolecular forces," *Colloids and Surfaces A: Physicochemical and Engineering Aspects*, vol. 293, pp. 229–240, 2007.

[28] L. Y. Yeo, O. K. Matar, E. S. P. de Ortiz, and G. F. Hewitt, "The dynamics of Marangoni-driven local film drainage between two drops," *Journal of Colloid and Interface Science*, vol. 241, no. 1, pp. 233–247, 2001.

[29] T. Gambaryan-Roisman, "Dynamics of free liquid films during formation of polymer foams," *Colloids and Surfaces A: Physicochemical and Engineering Aspects*, vol. 382, pp. 113–117, 2011.

[30] A. A. Mikhailovskaya, B. A. Noskov, S.-Y. Lin, G. Loglio, and R. Miller, "Formation of protein/surfactant adsorption layer at the air/water interface as studied by dilational surface rheology," *The Journal of Physical Chemistry B*, vol. 115, no. 33, pp. 9971–9979, 2011.

[31] V. B. Fainerman, S. A. Zholob, M. Leser, M. Michel, and R. Miller, "Competitive adsorption from mixed nonionic surfactant/protein solutions," *Journal of Colloid and Interface Science*, vol. 274, no. 2, pp. 496–501, 2004.

[32] C. Kotsmar, V. Pradines, V. S. Alahverdjieva, E. V. Aksenenko, V. B. Fainerman, V. I. Kovalchuk, J. Krägel, M. E. Leser, B. A. Noskov, and R. Miller, "Thermodynamics, adsorption kinetics and rheology of mixed protein-surfactant interfacial layers," *Advances in Colloid and Interface Science*, vol. 150, pp. 41–54, 2009.

[33] V. B. Fainerman, E. H. Lucassen-Reynders, and R. Miller, "Description of the adsorption behaviour of proteins at water/fluid interfaces in the framework of a two-dimensional solution model," *Advances in Colloid and Interface Science*, vol. 106, no. 1-3, pp. 237–259, 2003.

[34] R. Z. Guzman, R. G. Carbonell, and P. K. Kilpatrick, "The adsorption of proteins to gas-liquid interfaces," *Journal of Colloid and Interface Science*, vol. 114, no. 2, pp. 536 – 547, 1986.

[35] C. H. Chang and E. I. Franses, "Adsorption dynamics of surfactants at the air/water interface: A critical review of mathematical models, data, and mechanisms," *Colloids and Surfaces A: Physicochemical and Engineering Aspects*, vol. 100, pp. 1–45, 1995.

[36] A. F. H. Ward and L. Tordai, "Time-dependence of boundary tensions of solutions I. The role of diffusion in time-effects," *Journal of Chemical Physics*, vol. 14, no. 7, pp. 453–461, 1946.

[37] M. Durand and H. A. Stone, "Relaxation time of the topological $t1$ process in a two-dimensional foam," *Phys. Rev. Lett.*, vol. 97, p. 226101, Nov 2006.

[38] S. Ubal, C. H. Harrison, P. Grassia, and W. J. Korchinsky, "Numerical simulation of mass transfer in circulating drops," *Chemical Engineering Science*, vol. 65, no. 10, pp. 2934–2956, 2010.

[39] A. Sheludko, "Thin liquid films," *Advances in Colloid and Interface Science*, vol. 1, no. 4, pp. 391–464, 1967.

[40] N. D. Denkov, P. Cooper, and J. Y. Martin, "Mechanisms of action of mixed solid-liquid antifoams. 1. Dynamics of foam film rupture," *Langmuir*, vol. 15, no. 24, pp. 8514–8529, 1999.

[41] N. Politova, S. Tcholakova, K. Golemanov, N. D. Denkov, M. Vethamuthu, and K. P. Ananthapadmanabhan, "Effect of cationic polymers on foam rheological properties," *Langmuir*, vol. 28, no. 2, pp. 1115–1126, 2012.

[42] O. Reynolds, "On the theory of lubrication and its application to Mr. Beauchamp Tower's experiments, including an experimental determination of the viscosity of olive oil," *Philosophical Transactions of the Royal Society of London*, vol. 177, pp. 157–234, 1886.
[43] J. E. Coons, P. J. Halley, S. A. McGlashan, and T. Tran-Cong, "A review of drainage and spontaneous rupture in free standing thin films with tangentially immobile interfaces," *Advances in Colloid and Interface Science*, vol. 105, pp. 3–62, 2003.
[44] J. E. Coons, P. J. Halley, S. A. McGlashan, and T. Tran-Cong, "Bounding film drainage in common thin films," *Colloids and Surfaces A: Physicochemical and Engineering Aspects*, vol. 263, pp. 197–204, 2005.
[45] L. Wang and R.-H. Yoon, "Effects of surface forces and film elasticity on foam stability," *International Journal of Mineral Processing*, vol. 85, no. 4, pp. 101–110, 2008.
[46] A. M. Kraynik, "Foam drainage," Tech. Rep. SAND83-0844, Sandia National Laboratories, Albuquerque, New Mexico, USA, 1983.
[47] D. Vitasari, P. Grassia, and P. Martin, "Surfactant transport onto a foam lamella," *Chemical Engineering Science*, vol. 102, pp. 405–423, 2013.
[48] M. Mulqueen, K. J. Stebe, and D. Blankschtein, "Dynamic interfacial adsorption in aqueous surfactant mixtures: Theoretical study," *Langmuir*, vol. 17, pp. 5196–5207, 2001.
[49] K. Golemanov, N. D. Denkov, S. Tcholakova, M. Vethamuthu, and A. Lips, "Surfactant mixtures for control of bubble surface mobility in foam studies," *Langmuir*, vol. 24, pp. 9956–9961, 2008.
[50] D. Weaire and S. Hutzler, *The Physics of Foams*, ch. Foam Collapse, pp. 144–150. Oxford University Press, New York, 1999.
[51] A. Vrij, "Possible mechanism for the spontaneous rupture of thin, free liquid films," *Discussions of the Faraday Society*, vol. 42, pp. 23–33, 1966.
[52] D. S. Valkovska, K. D. Danov, and I. B. Ivanov, "Stability of draining plane-parallel films containing surfactants," *Advances in Colloid and Interface Science*, vol. 96, pp. 101–129, 2002.
[53] V. Bergeron, "Forces and structure in thin liquid soap films," *Journal of Physics: Condensed Matter*, vol. 11, pp. R215–R238, 1999.
[54] J. N. Israelachvili, *Intermolecular and Surface Forces*. Elsevier Science, 1985.